Application Note

HMI Rocker Switch With Hall-Effect Switches

Patrick Simmons *Current and Position Sensing*

ABSTRACT

There are numerous types of human machine interface controls. One in particular is the rocker switch. This often uses a mechanical connection to switch states. However, it is possible to achieve a similar output with Hall-effect switches. This document covers how that can be accomplished.

Table of Contents

List of Figures

List of Tables

Trademarks

All trademarks are the property of their respective owners.

1 Introduction

Working with complex machines such as vehicles, involves various tactile controls. Often these controls provide three states of operation, such as initiating a car door to lock, unlock, or remain idle and also when raising, lowering, or maintaining:

- window position such as found on a car door
- speed such as found in the cruise control of a car
- the volume of the radio

In addition to these, there are likely many more possible applications and these need not be strictly relevant to an automobile. One particular type of tactile control that can be utilized for such state selection is the *Rocker Switch*. This document dives into the basic operating principles and shows the design process for one possible version of a rocker switch. Challenges in the design process are also documented.

Figure 1-1 summarizes the design flow presented in this document.

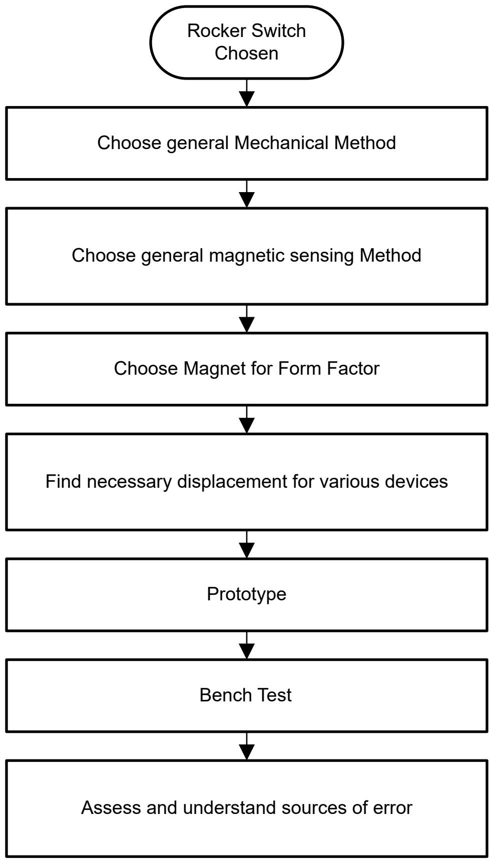

Figure 1-1. Design Flow

2 Design Process

2.1 Mechanical Implementation

Typically, the design begins with defining a system that executes a particular set of actions. In this case, the goal is a three-state switch in which there are two action states achieved when the user applies some force and another resting state, when the user applies no force or returns the switch to the default position. This actually might be achieved with multiple different styles of switch and is therefore subjective to the user preference, aesthetic, space, or cost. Figure 2-1 shows three possible mechanical options. This document explores what is necessary to make a three-state switch with the bottom option, the rocker switch.

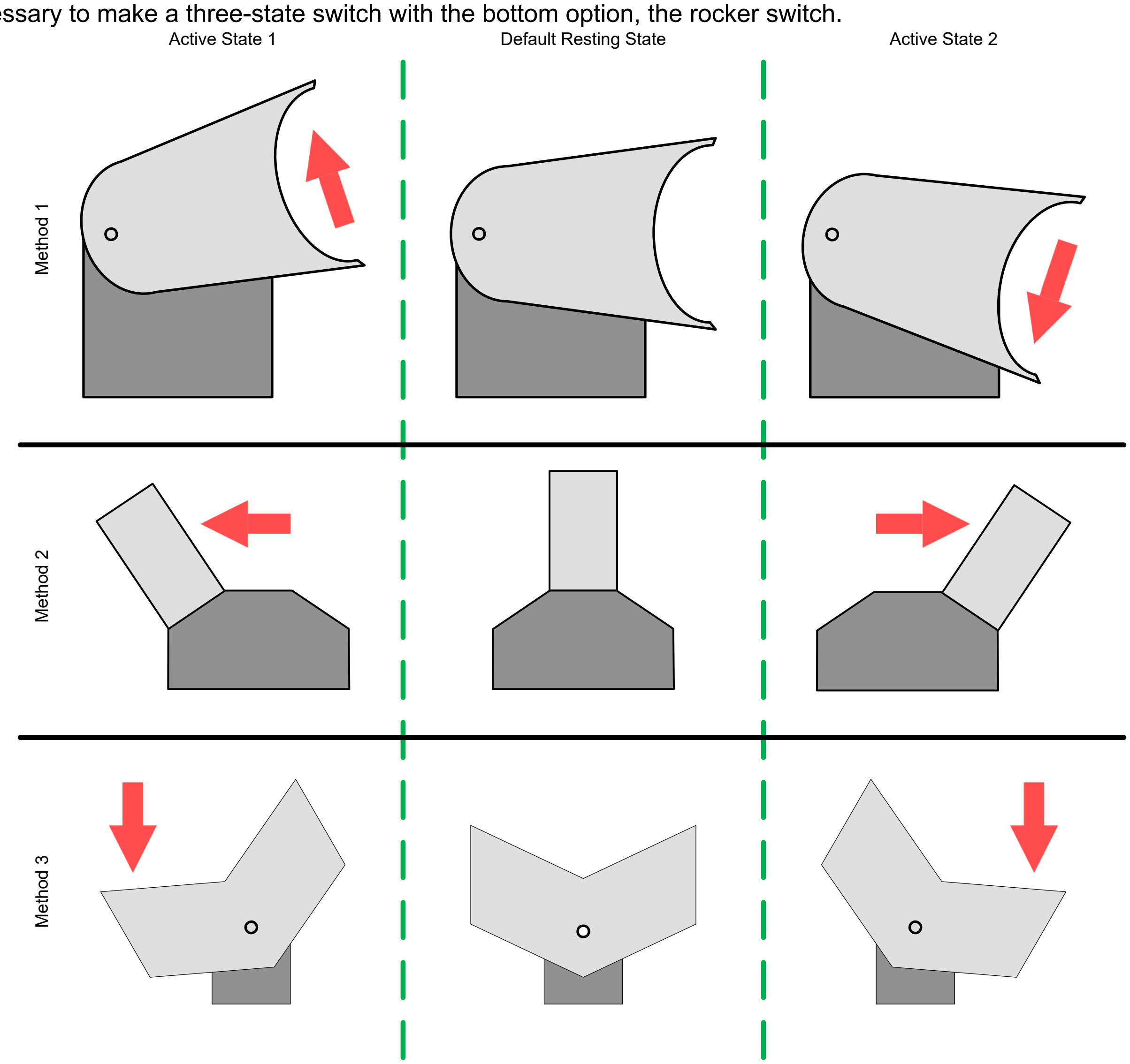

Figure 2-1. Mechanical Options

A rocker switch can be generalized into four basic mechanical components: a base, axle, springs, and a rocker. In this case the base holds the axle and has cantilevers that serve as springs for returning the rocker back to the resting state when the user is not applying force. While these cantilevers are not the primary focus in this design, note that traditional metal spring alternatives were intentionally avoided as many are typically composed of iron which can influence the magnetic field shape from a nearby magnet and thereby complicate design.

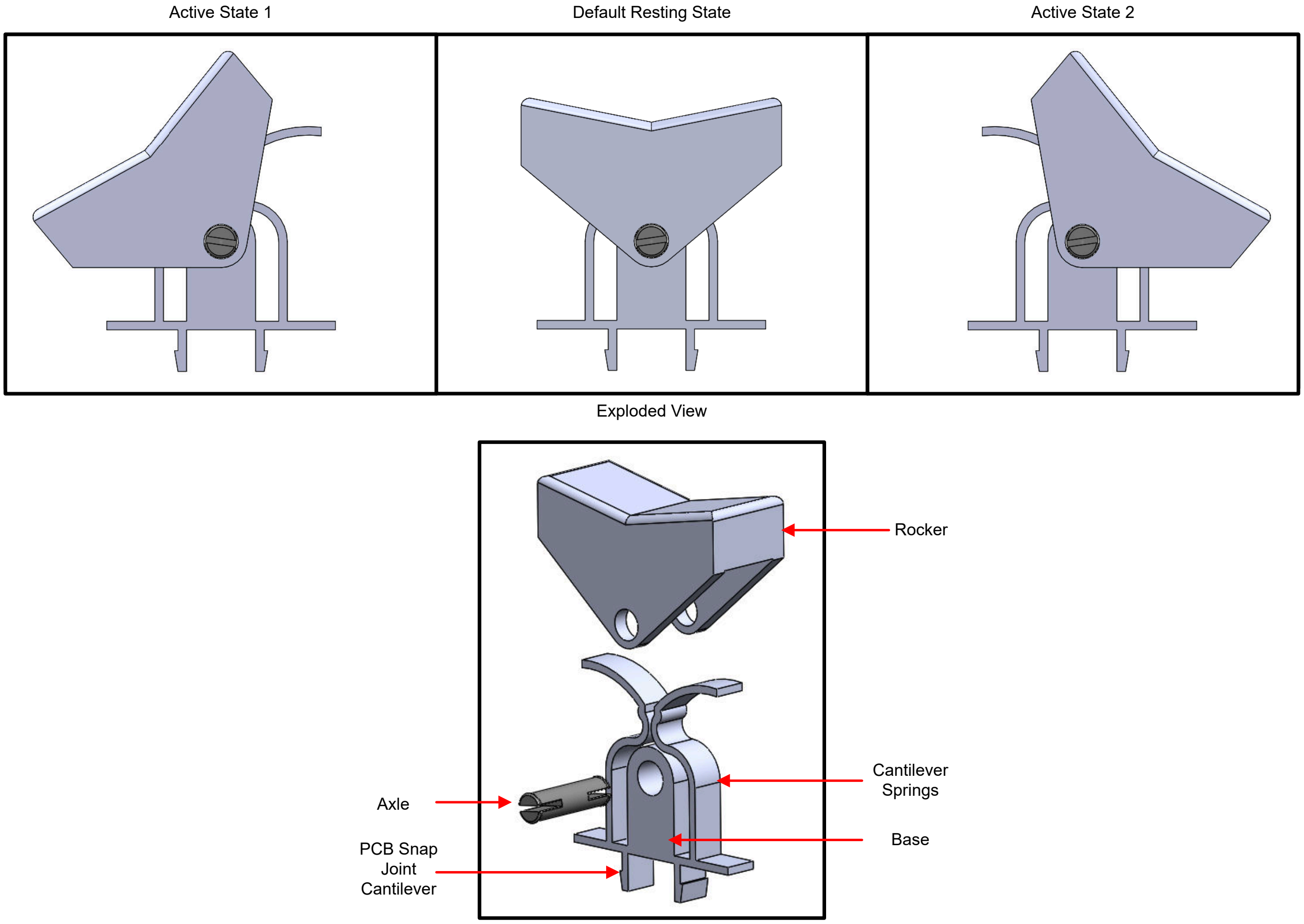

Figure 2-2. Mechanical Implementation

2.2 Magnetic Implementation

Upon choosing a style or mechanical implementation of the switch, consider how to transduce the mechanical stimulus into an electrical signal utilized by the system. Hall-effect sensors, especially Hall-effect switches, are a great option. Figure 2-3 illustrates the basic operation of an omnipolar Hall-effect switch. The image shows that a Hall-Effect switch has binary states of high and low, with the typical Hall-effect switch asserting low when the magnitude of the sensed magnetic field exceeds the B_{OP} threshold and the Hall-effect switch re-asserting high when the magnitude falls below the B_{RP} threshold. We can generalize that a magnet will trigger the Hall-effect switch low when it approaches and then trigger the Hall-effect switch high when it departs. However, the distance at which these triggers occur depends largely on the magnet specifications, the Hall-effect switch specifications, switch orientation, magnet orientation, and the displacement distance between the magnet and Hall-effect switch.

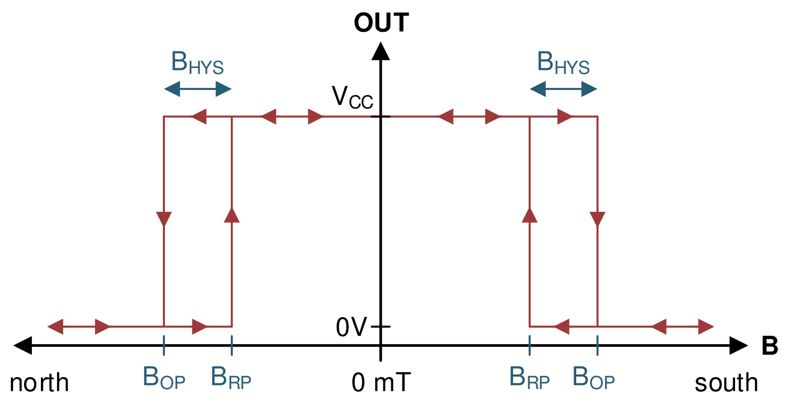

Figure 2-3. Omnipolar Behavior

As noted, device orientation does matter. While there are 3D Hall-effect sensors like the TMAG5170 and TMAG5273, Hall-effect switches do not sense magnetic fields in all directions and not all Hall-effect switches sense magnetic fields in the same direction. Figure 2-4 shows some examples of how a Hall-effect switch senses a magnetic field. In the left example is a typical surface mount SOT-23 Hall-effect sensor that senses in the z-direction like the TMAG5231. In the middle is another SOT-23 like the TMAG5123 that senses magnetic fields parallel to the package in the x or y direction. Lastly on the right is a typical through-hole TO-92 that senses in the x or y direction like the DRV5032AJLPG.

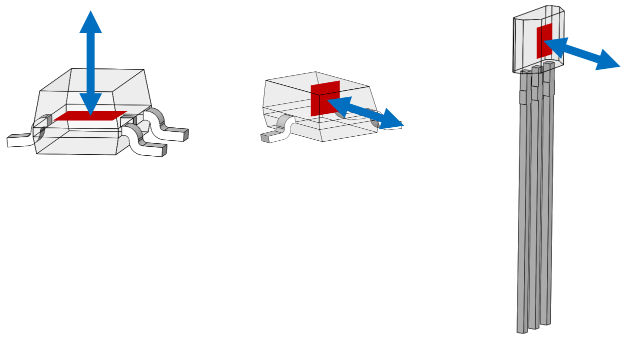

Figure 2-4. Sensing Axes

To better understand how relative magnet orientation and displacement affect sensor detection, examine the B-field of the block magnet in Figure 2-5. From this figure a few useful high-level concepts are derived. Points 1 and 2 correspond to the exit and entry points for the magnetic field radiating from the surface of the magnet. As the field enters from all 360° in the xy plane, these points see a strong field magnitude, purely oriented in the z-axis. As we move away from the points we see that the magnetic field begins to wrap around traveling from the North pole to the South pole. Consequently, as the direction of the field changes, we can expect that only a fraction of the field will be oriented in the z-direction and furthermore as the field lines do not converge at these other locations, the total field will be less than what is at points 1 and 2. Additionally, the longer the path the magnetic flux must travel from North to South, the greater the reluctance resisting the radiation of magnetic flux and the weaker the magnetic field (signified by the thinner field lines). With this basic understanding of the field pattern of the magnet and the relative field strength at various locations in space some reasonable assertions can be made on how the magnet and sensor should be oriented within the rocker switch.

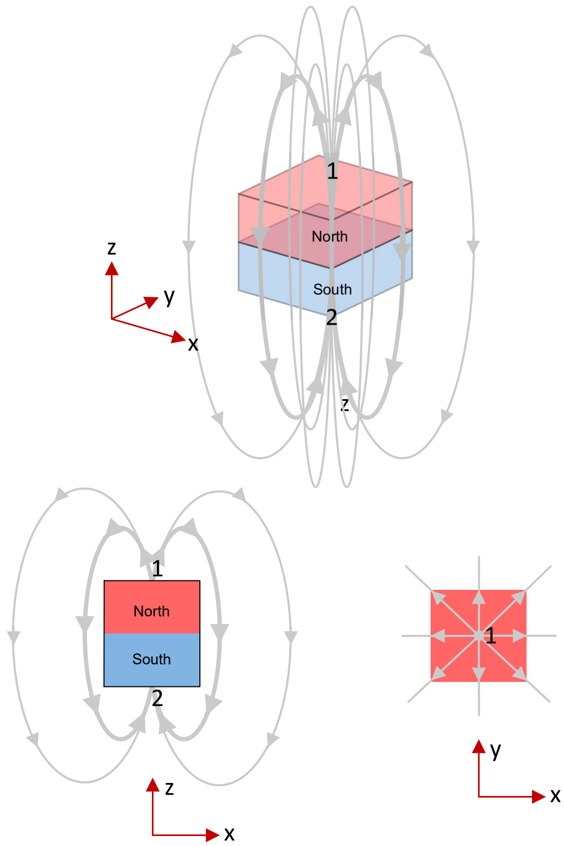

Figure 2-5. Magnet Field Lines

Equipped with this basic understanding of Hall-effect sensing direction and the field characteristics of a magnet, various general methods can now be formulated for the end goal. The end goal is to transduce our mechanical action into a system response through the following steps. The mechanical action is transduced into a field change sensed by our Hall-effect switch. Subsequently the Hall-effect switch translates this magnetic signal into an electrical signal. The electrical signal from the output of the Hall-effect then prompts some reaction from an actuator or microprocessor.

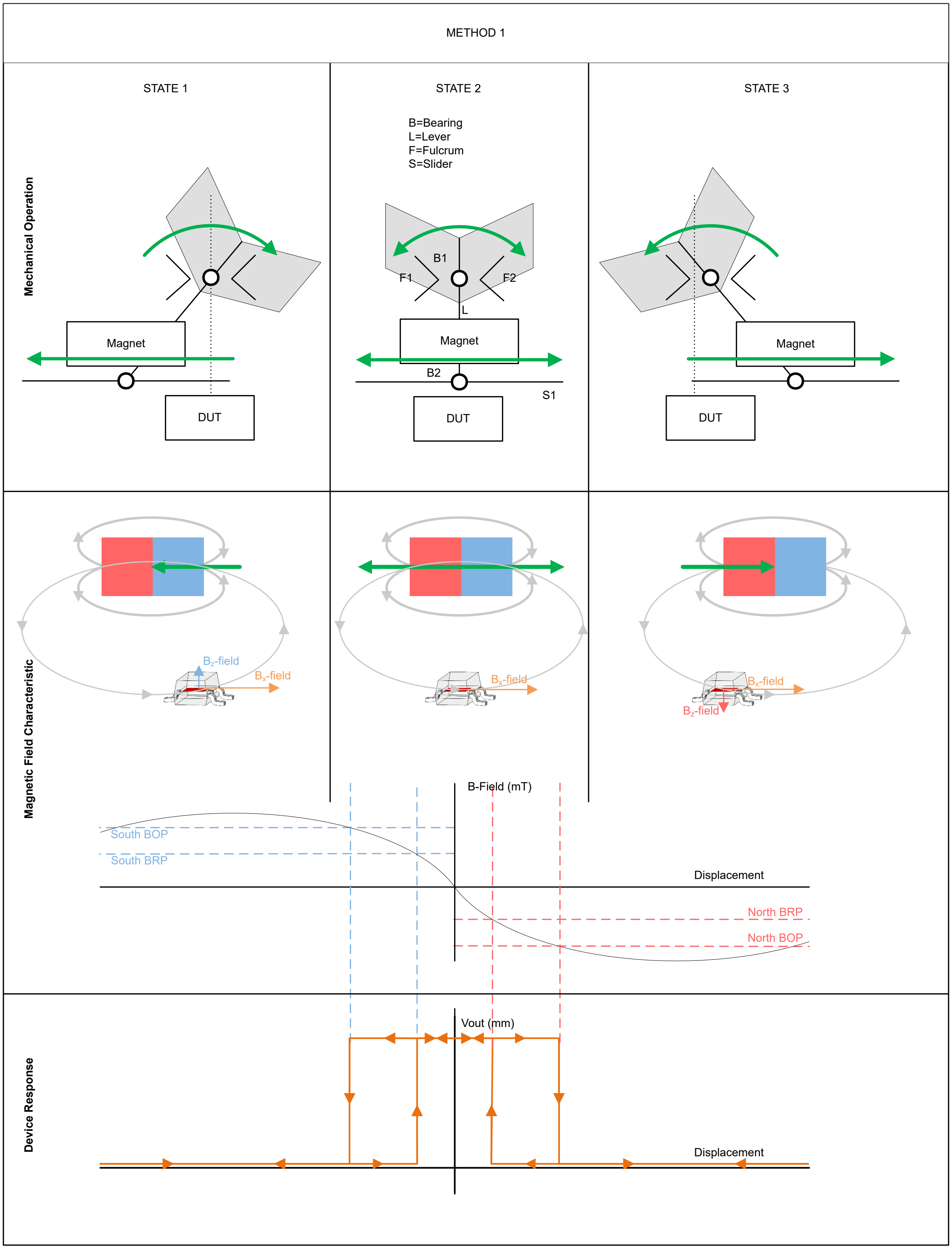

Figure 2-6. Method 1

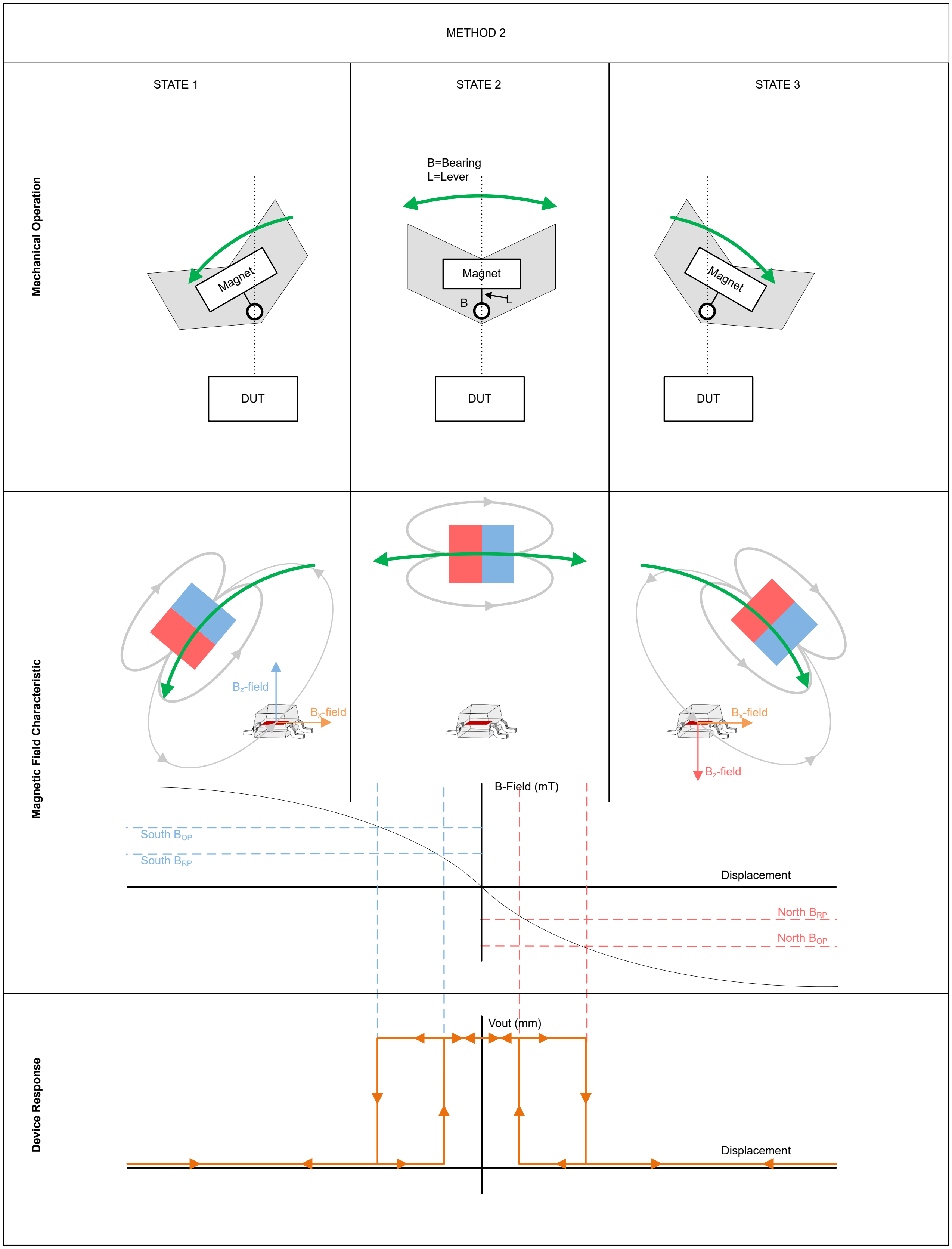

Figure 2-7. Method 2

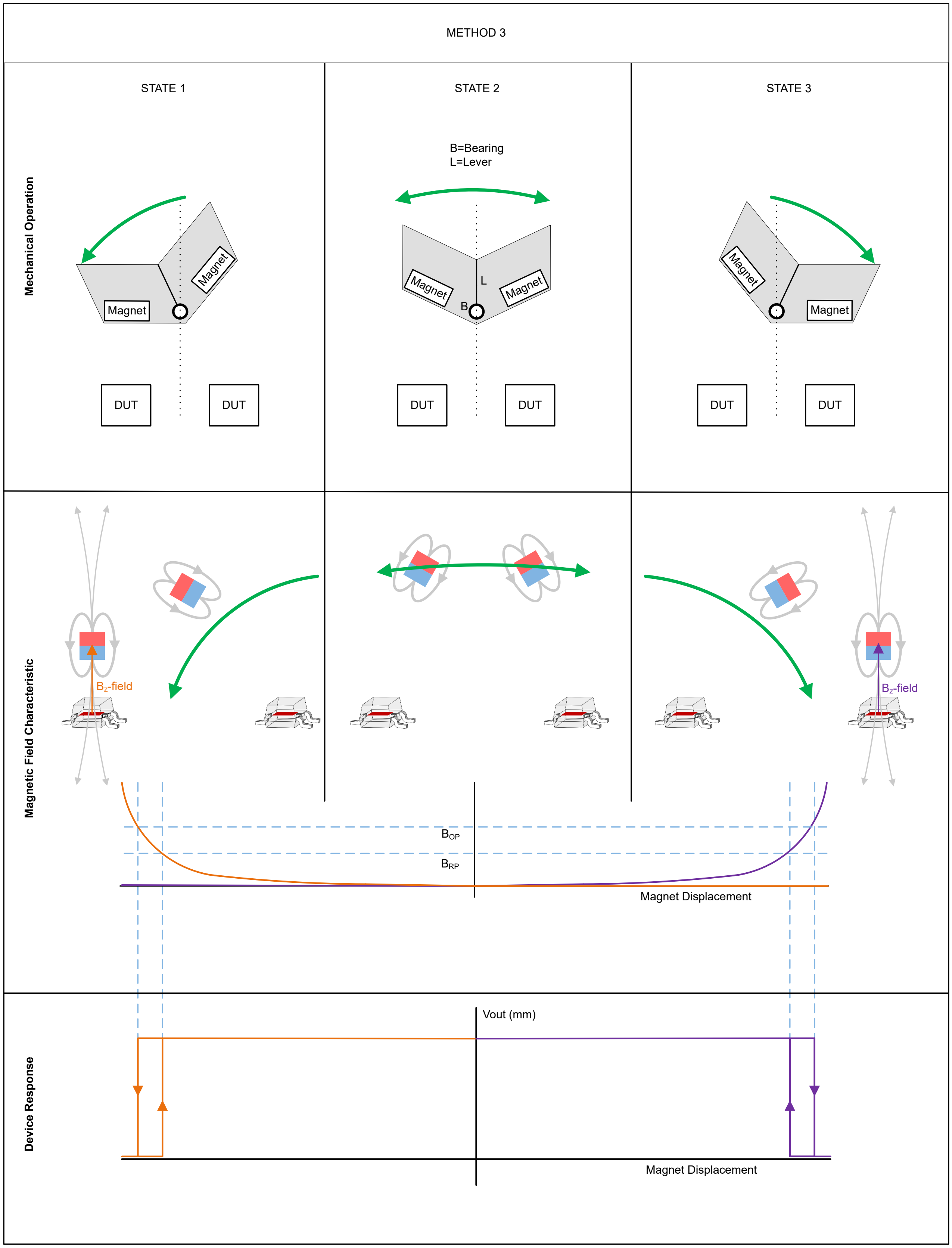

Figure 2-8. Method 3

One key detail seen in Figure 2-6 and Figure 2-7 is that only one sensor is used. When looking at a typical Hall-effect sensor data sheet, most devices have only one output. This typical device output may be unipolar and only capable of detecting a strong field oriented away from the device, or it might be omnipolar and incapable of distinguishing a strong field oriented away or toward the device. Despite this typical behavior, Texas Instruments does offer the DRV5032DU which has two unipolar outputs that detect the magnitude for opposing polarities as Figure 2-9 shows. This is the only device that could be used for these configurations.

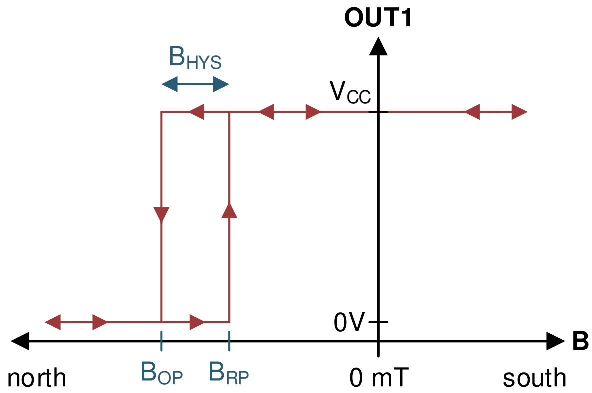

Figure 2-9. Dual Unipolar Behavior

As options 1 and 2 may require more mechanical design iteration and are appropriate for only one device that is not automotive qualified, this discussion proceeds with the method in Figure 2-8. A typical TO-92 option could be used, but this design uses a SOT-23 that senses in the z-axis normal to the top of the package and the PCB.

2.3 Magnet Sensor Placement

As a rocker switch will likely have a small form factor with its structure obscuring the magnet from the view of the end user, the magnet will likely be small and the smaller the magnet the weaker its field strength. As previously alluded to, offsets further from the magnet have weaker fields. Consequently, to have the device see the maximum field, align the magnet center to the Hall element center of the DUT when the switch is fully engaged and the magnet is parallel to the DUT.

To quickly get an idea of what might trigger the device, select a magnet that will fit within the switch structure shown in Figure 2-10 and run some calculations or simulations to see what distance is required. For calculations, leverage TI's Magnetic Sensing Proximity Tool. At the time of this writing, the smallest non-custom magnets readily available that are reasonably sized for the intended switch are Neodymium N42 magnets, which come in a form factor well below an inch. The smallest magnet found is 1/8 in × 1/8 in × 1/16 in (3.175 mm × 3.175 mm × 1.5875 mm). N42 is a quite strong magnet and several Hall-effect switches have trigger thresholds in the low mT range. Particularly, the B_{RP} minimum threshold may be as low as 0.5 mT. This immediately raises the question of whether the rocker can move sufficiently far away in the rest state to fall below the B_{RP} threshold.

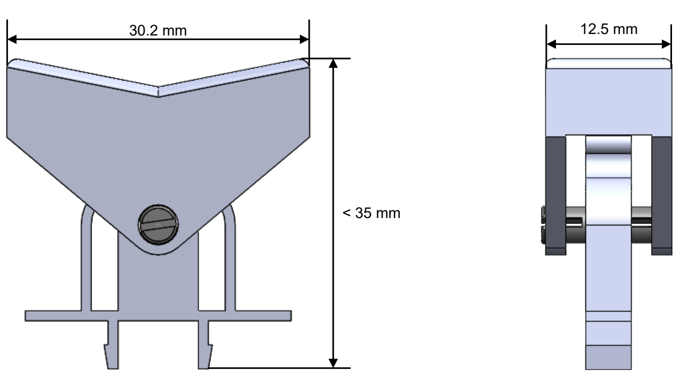

Figure 2-10. Rocker Size Constraints

Because the magnet moves in an arc, the hinge option for magnet movement is used in the tool. Subsequently, an educated guess is made on what might work within the bounds of the manufactured mechanical switch. Therefore, magnets and Hall-effect switches are placed at the locations indicated in Figure 2-11. This configuration is used because the modeled part can be quickly revised with parameterized dimensions in two locations, A and B. With TI's Magnetic Sensing Proximity Tool, dimension A corresponds to *Sensor Z-offset* + device height (assumed to be 1.12 mm) while dimension B corresponds to *Magnet Z-offset* multiplied by –1 (due to the tool offset being based on the z-axis rather than the x-axis). Both of the dimensions are relevant to the hinge axis, which is the center of rocker switch axle. The final dimension is C, and this corresponds to the *Arc Radius*. This dimension is constrained by the desired switch width in the resting state. To simplify the design iterations, 13.5 mm is assumed.

Magnet Characteristics		
L	3.18	mm
W	3.18	mm
T	1.59	mm
Magnet Material	N42	
Br (Remanence)	13000	G

Displacement Dimensions		
a1	0	degrees
a2	45	degrees
X-Offset	0	mm
Y-Offset	0	mm
Sensor Z-Offset	-8.450	mm
Magnet Z-Offset	1.210	mm
Arc Radius	13.500	mm

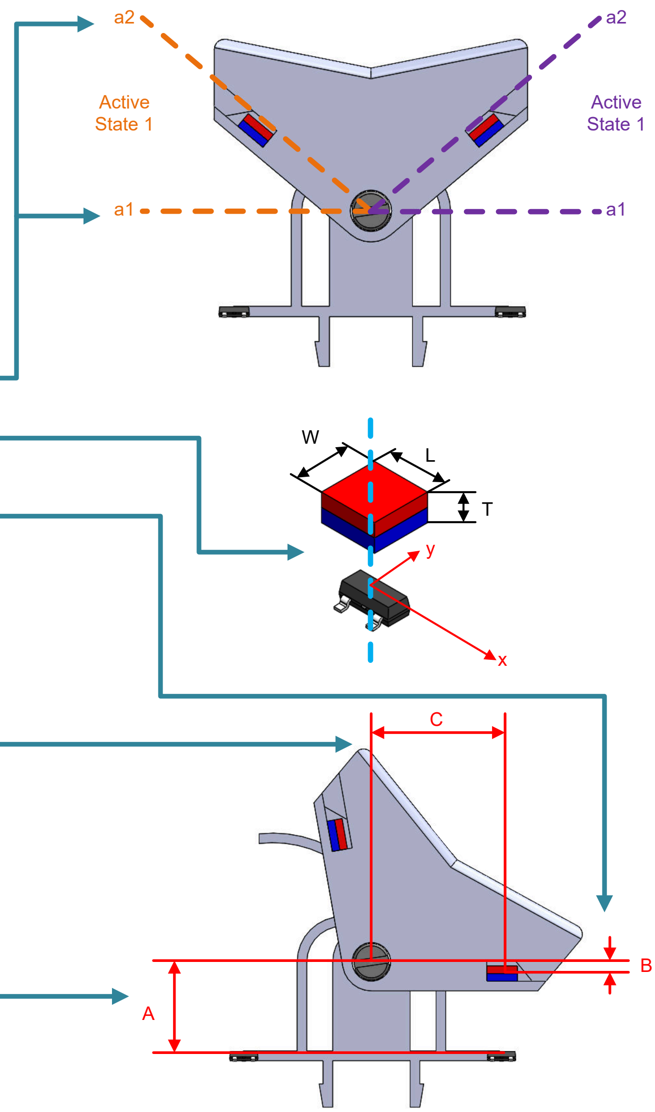

Figure 2-11. Setup

To use TI's Magnetic Sensing Proximity tool, a valid supply voltage value must still be entered, along with a type of device, and a device. A valid supply voltage is any voltage that is within the recommended operating range of at least one device in Texas Instrument's Hall-effect position sensing portfolio. A voltage of 5 V would be reasonable here, but up to 38 V can be used for automotive-grade parts. As for the type of device, enter unipolar or omnipolar switch; however, keeping track of the polarity of the magnet for omnipolar switches is less necessary and therefore can simplify the manufacturing process. Upon selecting a device, the tool provides the option of selecting a package based upon the postfix of each specific part. Because a surface mount SOT-23 is used, look for part names ending in *DBZ*.

Having an automotive qualified offering, the DRV5033FAQDBZ is a reasonable first device to assess. The goal is to find the appropriate part and corresponding parameters in which B_{OP} max and B_{RP} min are bounded within a1 and a2 as shown in the middle graph in Figure 2-12. Ensuring B_{OP} max and B_{RP} min are within bounds, accounts for device variation and temperature drift in the design as the B_{OP} and B_{RP} thresholds for the device can deviate from the typical value, and in the worst case could be at the maximum or minimum values. If the field is too strong, the output graph will look similar to the left graph and it is possible some devices in the mass production of the system might not trigger high. Alternatively if the field is too weak, the tool voltage output graph will look like the right and some system production devices may never trigger low.

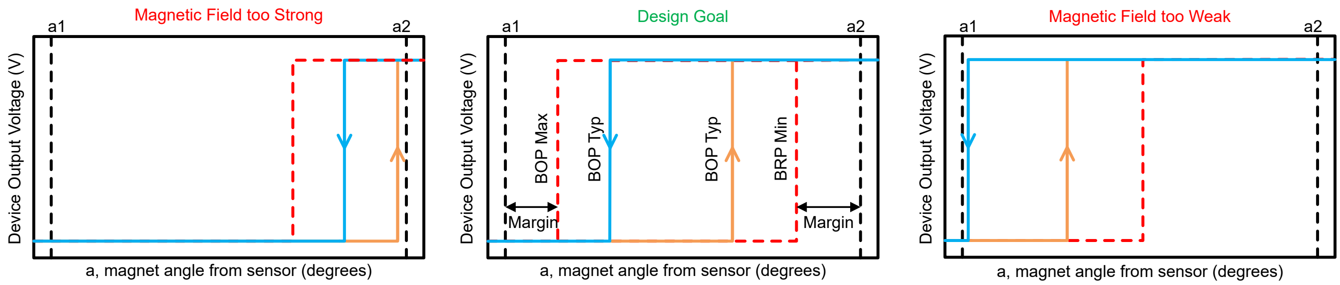

Figure 2-12. Example Plots

After a few iterations of manipulating the Sensor Z-Offset and the Magnet Z-Offset, suitable values were found that work according to the tool as indicated in Figure 2-13.

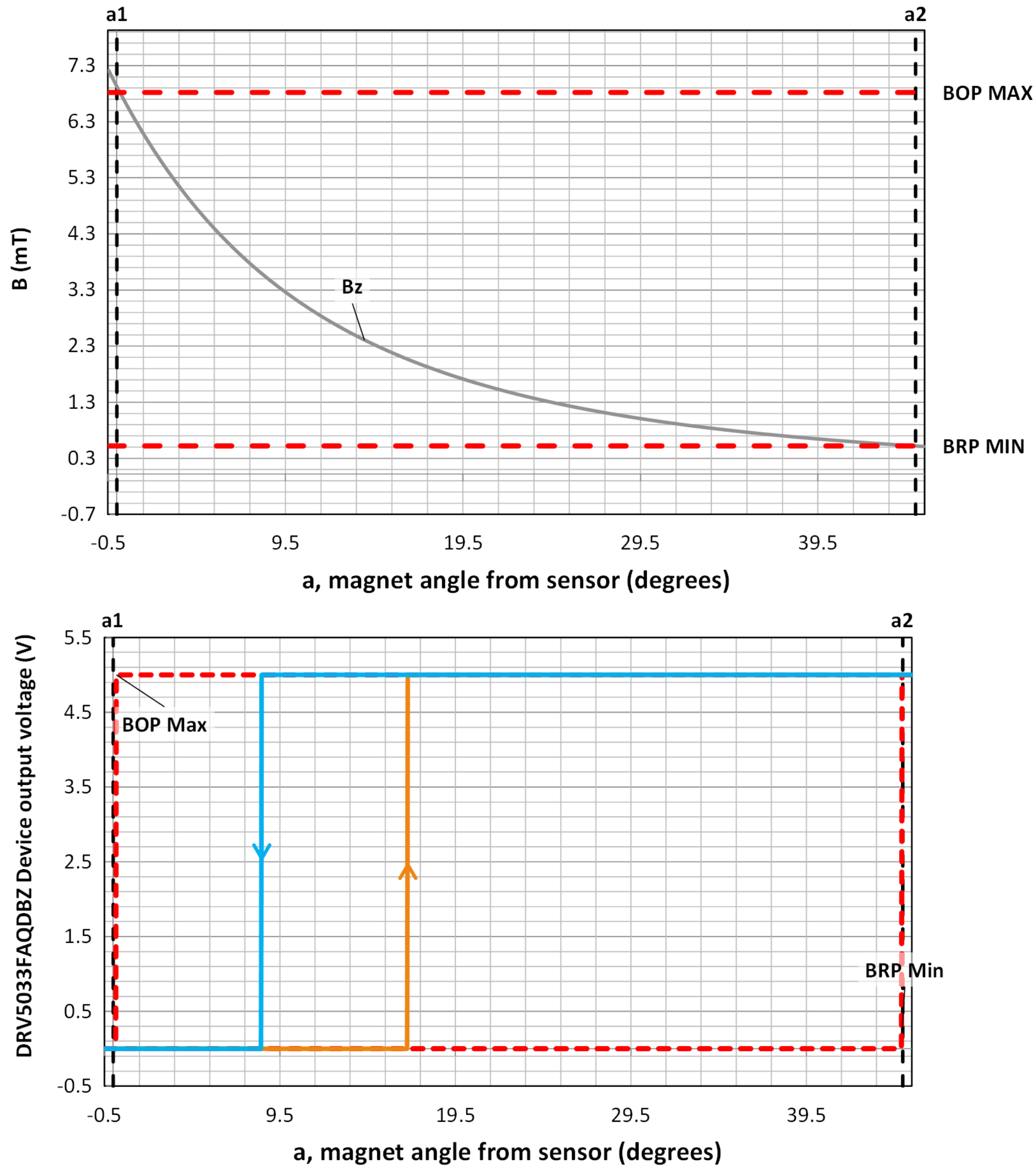

Figure 2-13. DRV5033FA Preliminary Analysis

As Figure 2-13 shows, the device should trigger low just before the rocker reaches 0° for one of the active states and it should trigger high just before 45°, the boundary of the resting state. While this is good and accounts for device variation and temperature drift, it still does not provide a lot of margin, which might be necessary for system manufacturing tolerance. With system manufacturing tolerance the magnet may be offset in the mechanical switch structure, the Hall-effect switch may be offset on the PCB, or mechanical switch may be offset on PCB. With this in mind, a little more design margin is desirable and a different sensitivity variant, the DRV5033AJQDBZ with higher B_{OP} and B_{RP} thresholds, should be considered. The motivation for this is that a much smaller change in range would be required to trip both thresholds when considering the B-field graph characteristic. Figure 2-14 illustrates that an equal difference in B_{OP} and B_{RP} can have substantially different mechanical ranges depending on how high the thresholds are. If the magnet can be moved close enough to our Hall-effect switch, the field will be much stronger and the spatial hysteresis range for devices with relatively equivalent B_{hys} specifications will be much smaller.

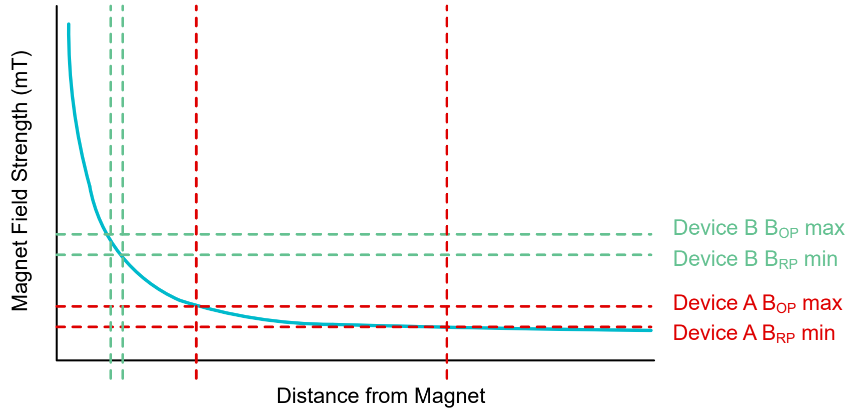

Figure 2-14. Transition Regions

After manipulating the sensor Z-offset variable some, a small improvement is seen in the margin as shown in Figure 2-15. This small improvement is not too surprising because the B_{RP} minimum is only 0.5 mT higher and the typical hysteresis is larger for the DRV5033AJ.

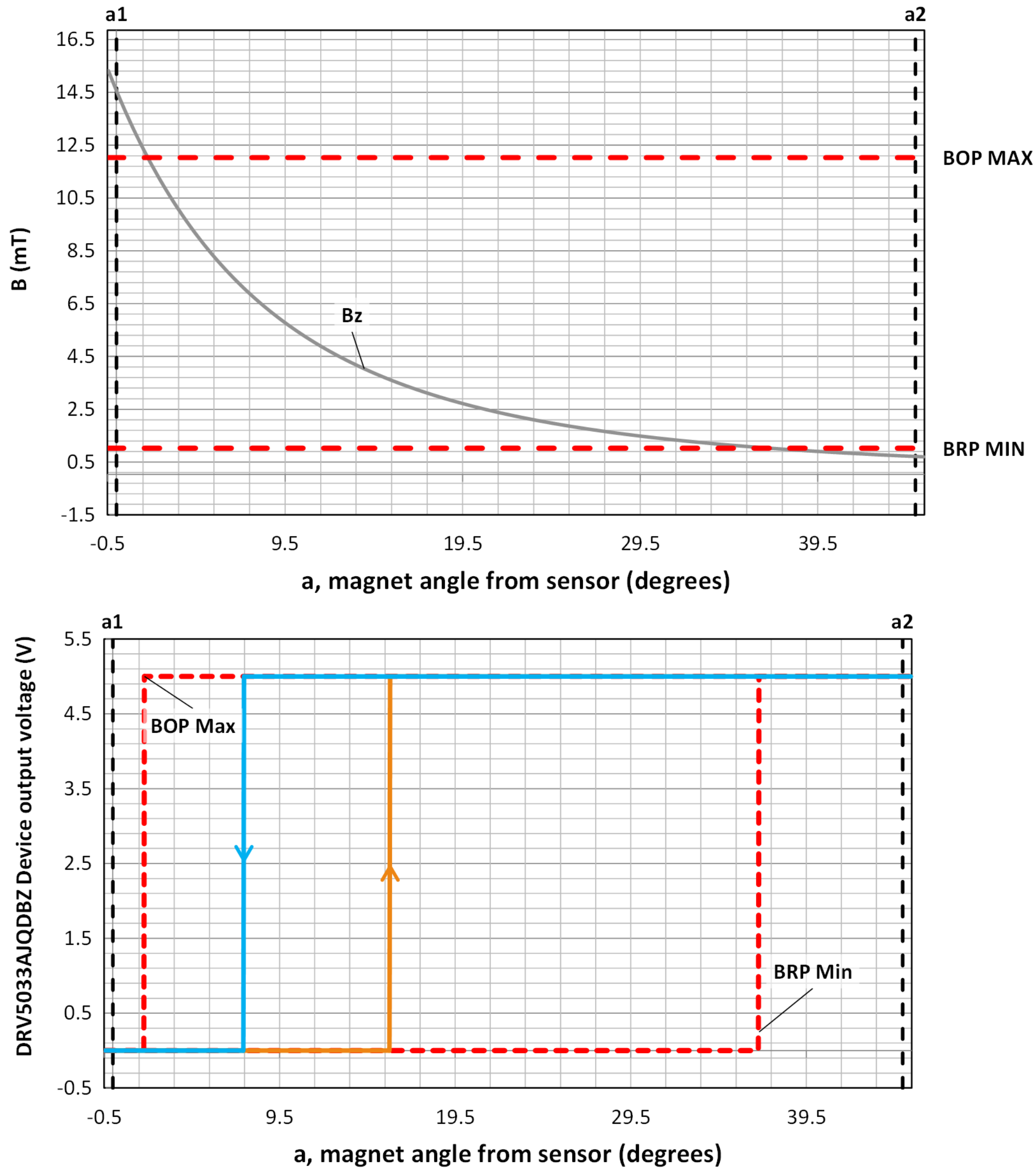

Figure 2-15. DRV5033AJ Preliminary Analysis

Consequently, another part is evaluated, the DRV5032ZEDBZ, which presently has the highest switch thresholds in the TI Hall-effect sensor portfolio with a B_{OP} maximum of 63 mT and a B_{RP} minimum of 30 mT.

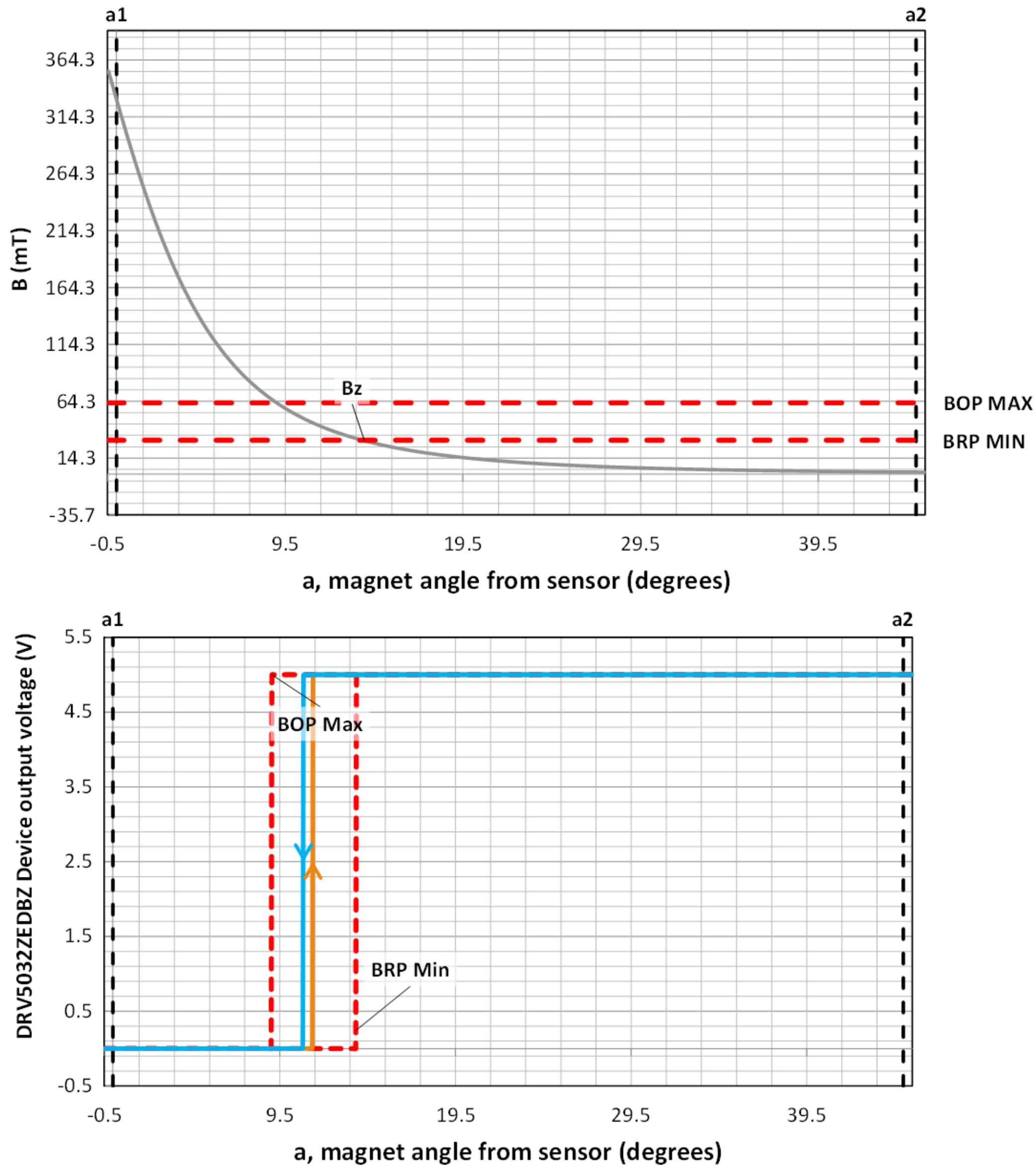

Figure 2-16. DRV5032ZE Preliminary Analysis

Figure 2-16 shows that the DRV5032ZE does seem quite promising. However, by exercising due diligence one problem is discovered. Because the magnet is small and a strong field is required, a low manufacturing tolerance must be assured. If the magnet x, y, and z offset tolerances are all +1.25 mm, then there might be systems in which the switch never triggers low as indicated in Figure 2-17. Consequently, if proceeding with this device, it might be a good idea to use a slightly larger magnet, with identical length and width dimensions, but a larger thickness.

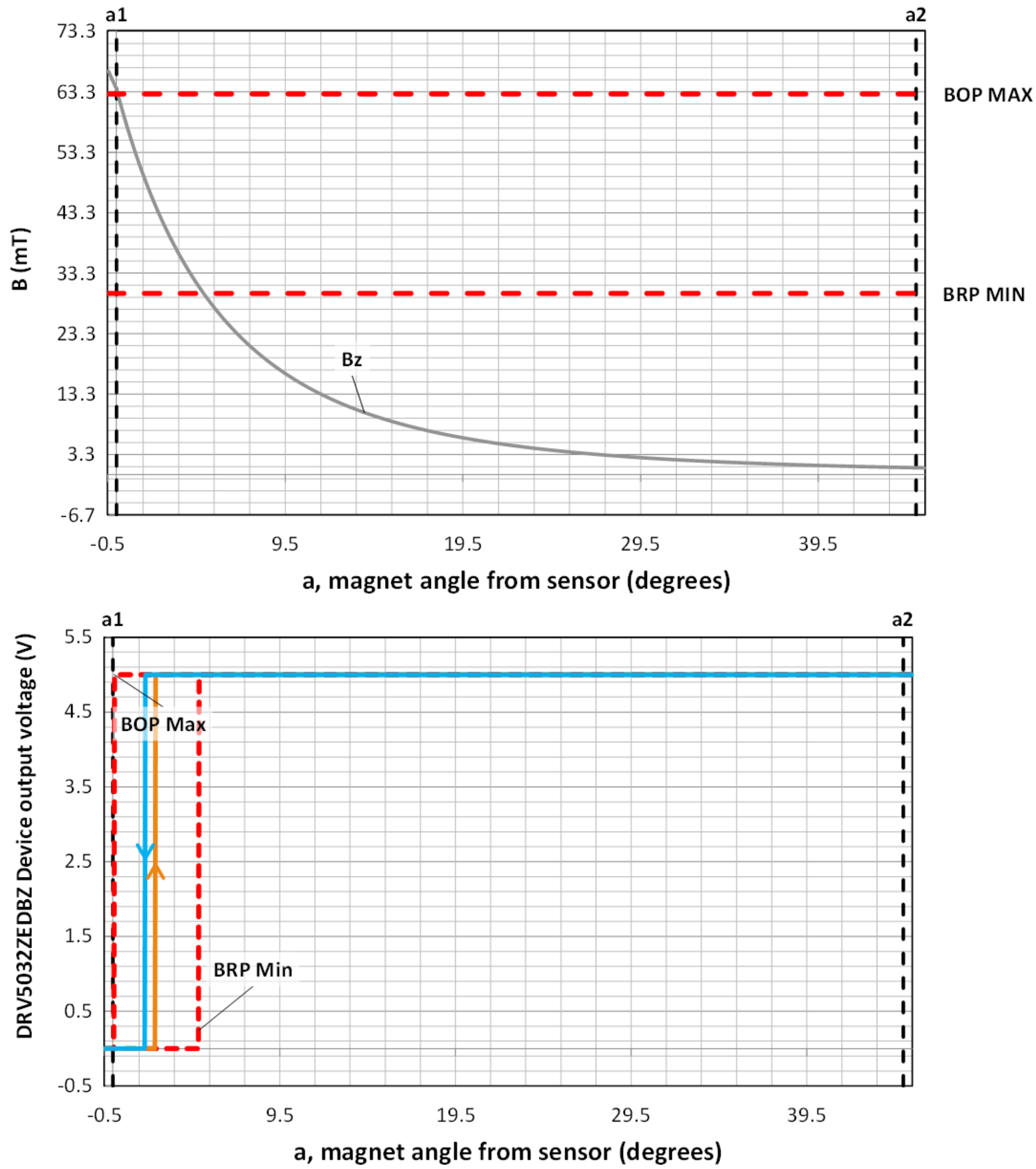

Figure 2-17. DRV5032ZE_Adjusted_Analysis

Table 2-1. Design Tool Entries

Specifications	DRV5033FA	DRV5033AJ	DRV5032ZE
Magnet Movement	Hinge	Hinge	Hinge
Magnet Shape	Block	Block	Block
Magnet Orientation	South Facing DUT	South Facing DUT	South Facing DUT
Magnet L	3.175 mm	3.175 mm	3.175 mm
Magnet W	3.175 mm	3.175 mm	3.175 mm
Magnet T	1.5875 mm	1.5875 mm	1.5875 mm
Magnet Material	N42	N42	N42
Br	13000 G	13000 G	13000 G
a1	0°	0°	0°
a2	45°	45°	45°
X-Offset	0 mm	0 mm	0 mm
Y-Offset	0 mm	0 mm	0 mm

Table 2-1. Design Tool Entries (continued)

Specifications	DRV5033FA	DRV5033AJ	DRV5032ZE
Sensor Z-Offset	–8.45 mm	-6.68 mm	–1.98 mm
Magnet Z-Offset	1.21 mm	1.21 mm	1.21 mm
Arc Radius	13.5 mm	13.5 mm	13.5 mm
V_{Supply}	5 V	5 V	5 V
Type of Device	DRV5033FAQDBZ	DRV5033AJQDBZ	DRV5032ZEDBZ

2.4 Prototyping and Bench Testing

Prototyping and Bench Testing

After the initial design comes the final crucial steps of prototyping, testing, and revising. As the tool approximates the B-field based on ideal conditions, try to compensate with all sources that can be identified at the time of the preliminary design. In the course of building the prototype, there may be undesirable aspects of how the switch moves, additionally, various error sources that were not initially accounted for may be discovered. These various issues become more obvious with a physical prototype. Figure 2-18 is the prototype that was designed for this application report.

2.5 Layout

The layout consists of four rocker switch locations placed similar to what might be seen in some automotive door window modules. Each location has two Hall-effect switches, one switch for active rocker lowered left and another for active rocker lowered right. With each rocker switch, there are 3 LEDs: two for the active states and one for the default inactive state. The inactive state LED is driven by an XOR that outputs low when both Hall-effect switch outputs are high.

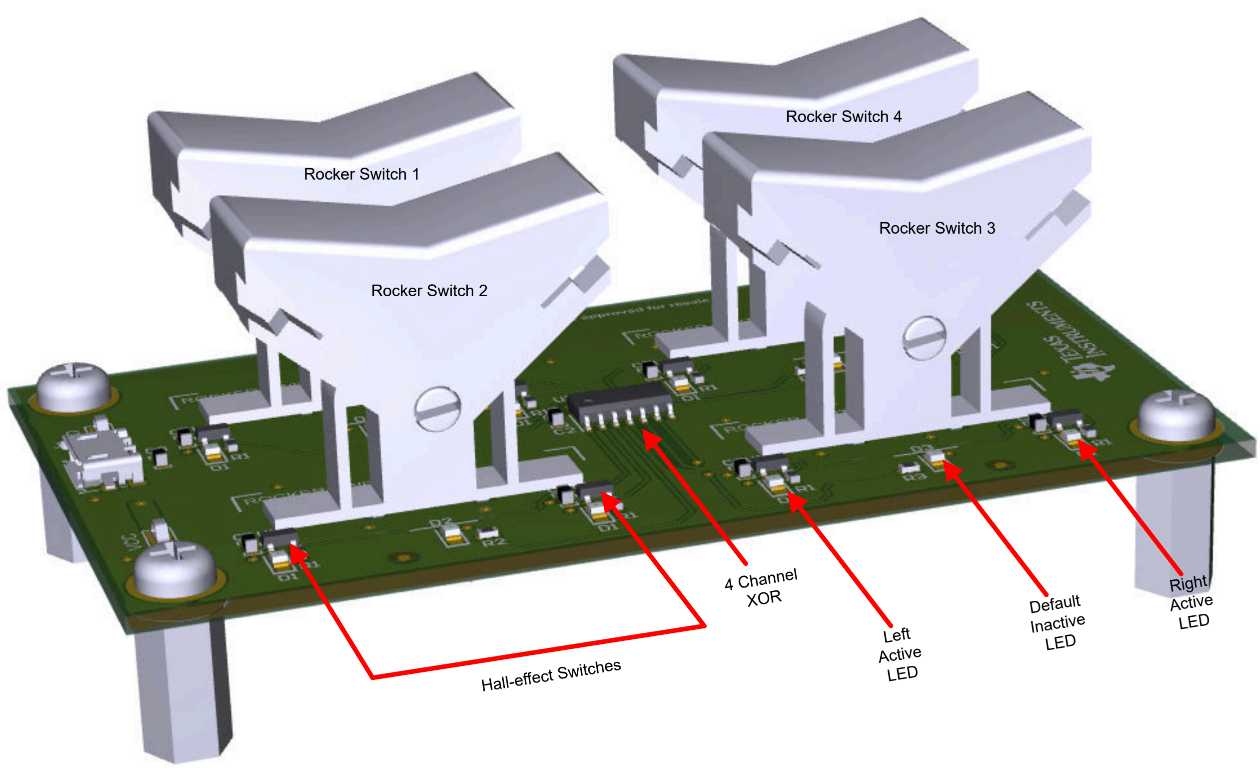

Figure 2-18. Rocker Switch Module

2.6 Bench Testing

To assess the performance of the rocker switch, side view videos were recorded to capture the on and off transition points of the LEDs designated for the corresponding default or active states. From these videos, the z and x coordinates of the hinge origin and triangle reference lines were recorded to derive the transition angle with a tangent function. Figure 2-19 shows one example. All of the bench tests were conducted at room temperature.

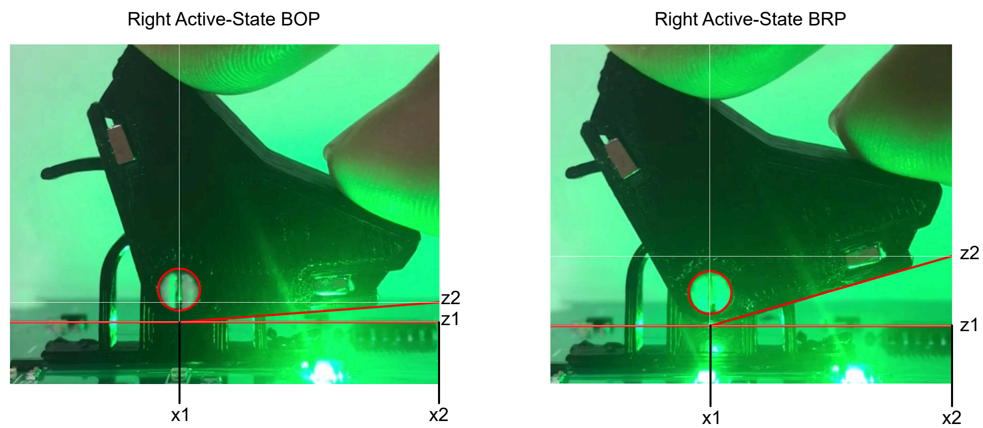

Figure 2-19. Bench Analysis Method

$$\text{angle} = \text{atan}\left(\frac{z_2 - z_1}{x_2 - x_1}\right) \quad (1)$$

2.7 Bench Results

After collecting all the data, assess whether the results make sense and possibly find explanations for inconsistencies. Ideally, all of the data falls within the expected measurement range based upon the threshold bounds calculated in the preliminary design phase. Such data could be assessed in a chart similar to Figure 2-20.

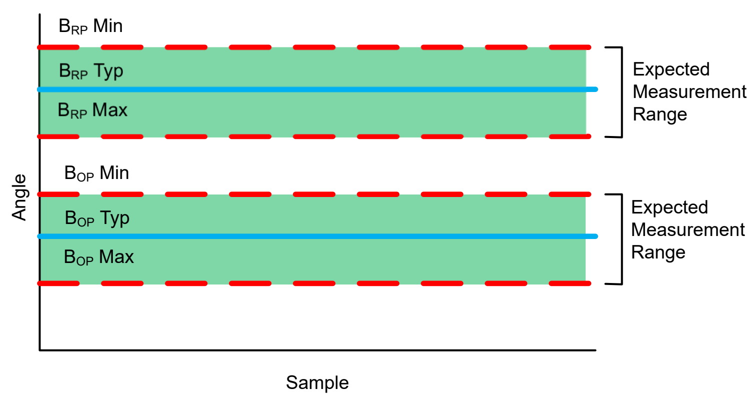

Figure 2-20. Acceptable Measurement Range

Figure 2-21 shows the results accumulated for three boards that each have one DRV5033FA-based rocker-switch, one DRV5033AJ-based rocker-switch, and one DRV5033ZE-based rocker-switch. Each rocker had two Hall-effect switches. Notice that some of the measured thresholds were not within the bounds suggested by the calculator tool. This is something to be expected when only Hall-effect switch variation and temperature drift is considered and the tolerances of the PCB and rocker switch structure have loose tolerances. After recalculating the B_{OP} maximum threshold with some reasonable offset of 0.5 mm for x, y, and z included, notice that the measurements logged are not too unreasonable. The *Error Sources* section delves into the various error sources and attempts to quantify their impact.

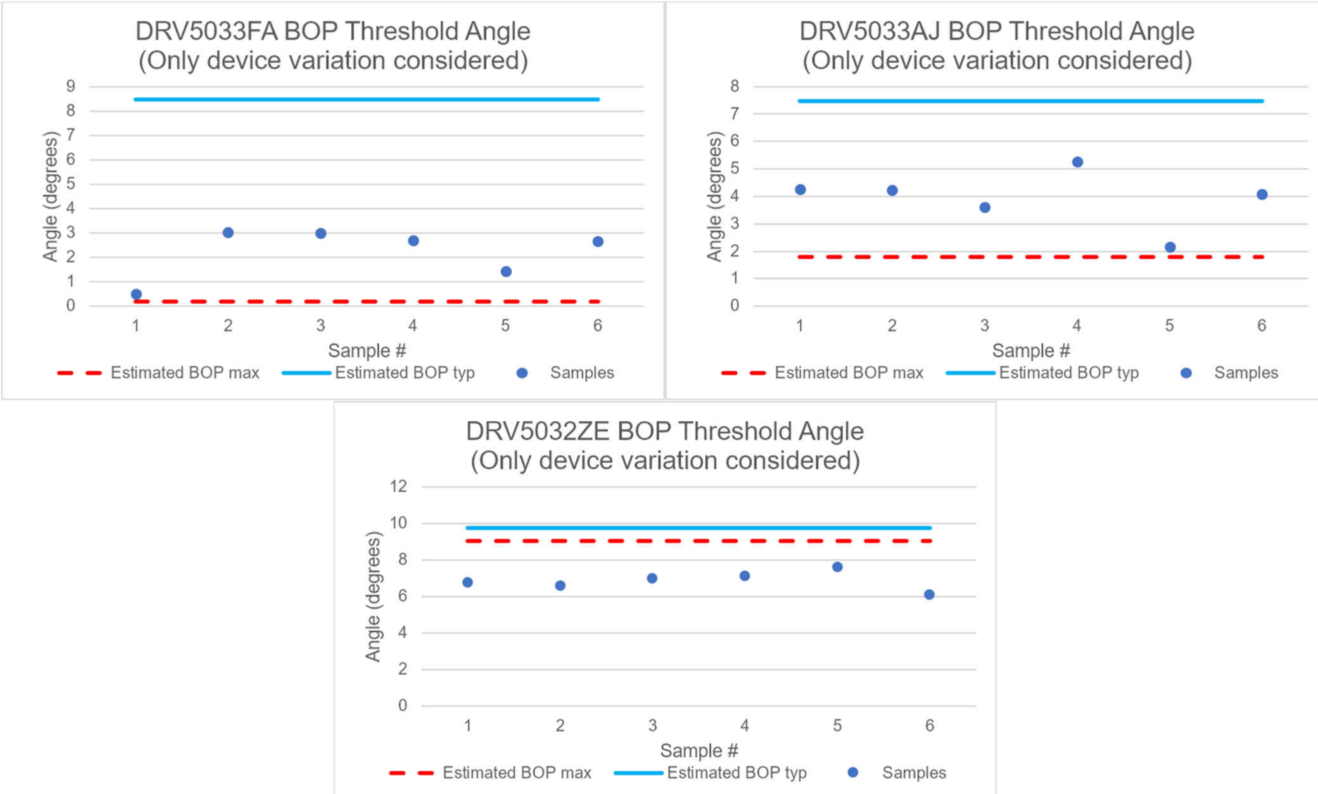

Figure 2-21. Bench Results vs Ideal Expectations

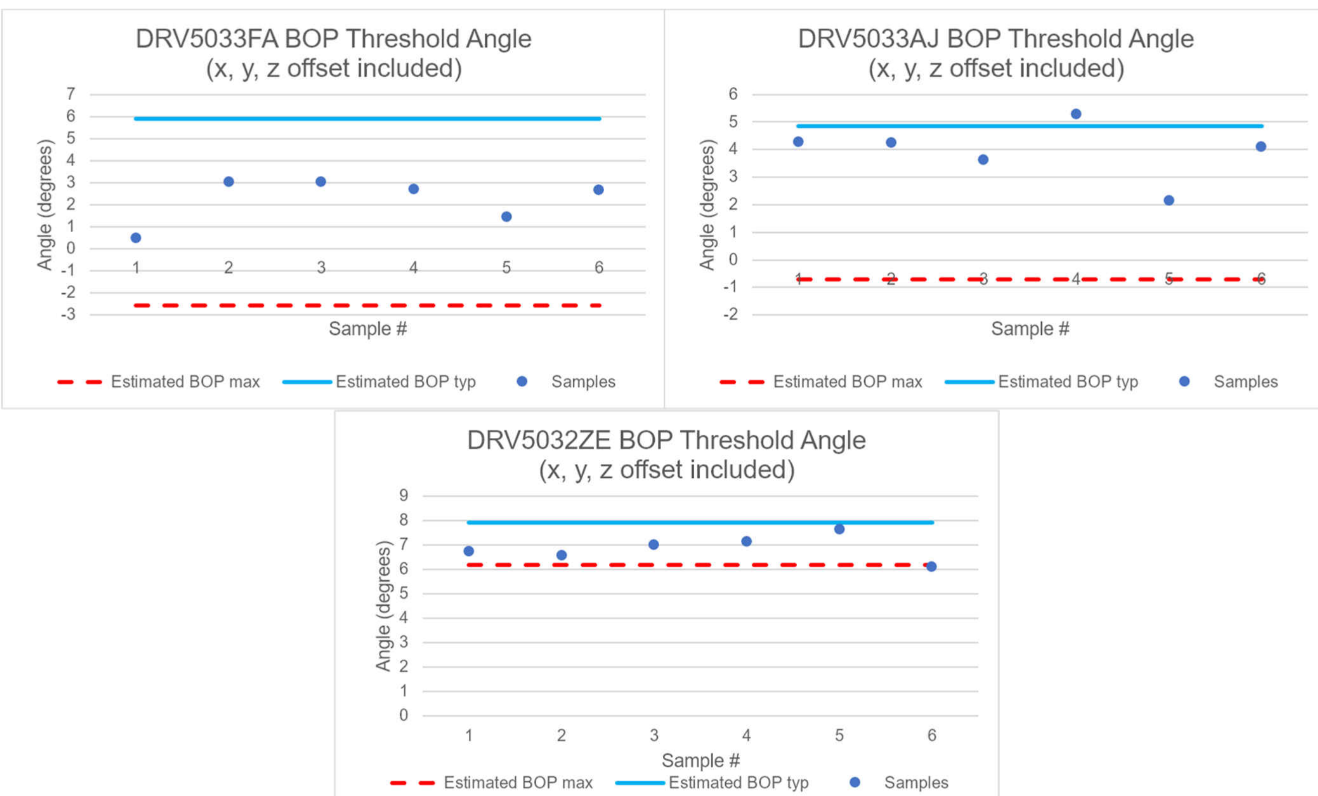

Figure 2-22. Bench Results vs Bounds Including Offsets

2.8 Error Sources

In the preliminary design, the error source primarily considered was device variation of B_{OP} and B_{RP} . However, there are several other sources of error, many of which correspond to fabrication and assembly. In the process of evaluating on the bench such error sources are easier to identify, thereby making bench testing a good and necessary practice to embrace before proceeding to mass production. The following list shows all possible error sources identified for this particular design including the ones accounted for in the preliminary design:

- Offsets
- Roll, Yaw, and Pitch
- Magnet Variation
- Device Variation and Temperature Drift
- External Fields
- Nearby Material Influence
- Bench Setup Error

2.8.1 Offsets

Offset corresponds to the displacement between the magnet and Hall-effect device, when the mechanical switch is oriented at the 0° angle. Figure 2-23 illustrates how offsets are defined in the calculator tool.

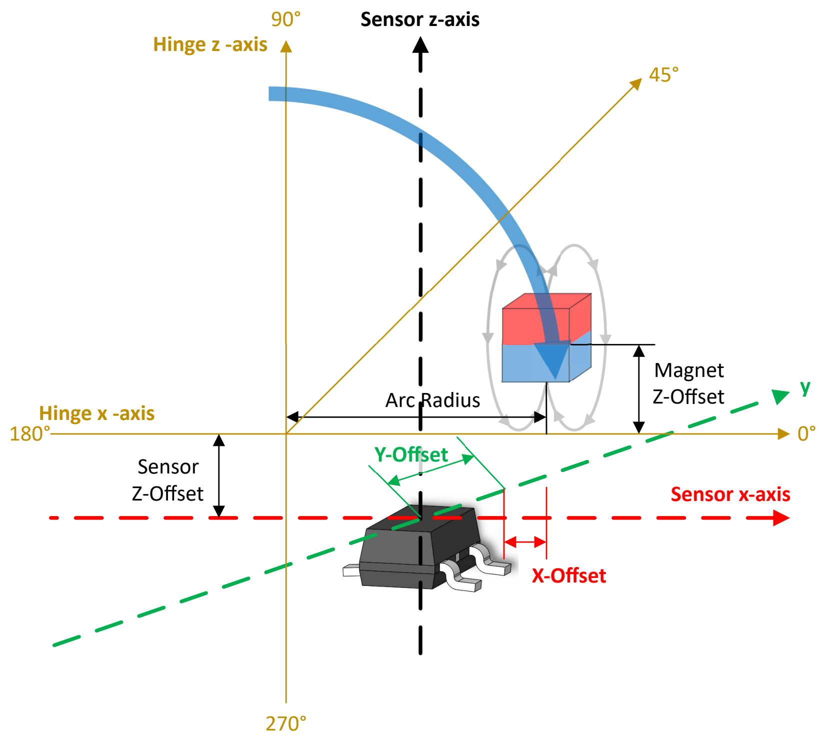

Figure 2-23. Displacement Offsets

The source of offset error can be attributed to PCB manufacturing and rocker assembly manufacturing. In the example documented in this note, while the PCBs were fabricated by a PCB manufacturer, the slots for the holding rocker were hand drilled. The rocker assembly was 3D printed, and the printer has a resolution of 0.0125 to 0.05 mm. Due to the level of precision when cutting the slots, there were notable instances in which the assemblies were a little off center and their bases not flush with the board. In addition to these manufacturing and assembly errors, there was also a z-offset error contributed by the tool. The tool assumes all SOT-23 packages are 1.12-mm tall and uses that value for calculating the surface to Hall-element offset. Post analysis revealed that some package heights were as low as 0.947 mm.

Large tolerances in the x-offset, y-offset, sensor z-offset, and magnet z-offset can all have a significant impact on the B-field detected at the DUT Hall element, especially when the magnet size is small. Figure 2-24 and Figure 2-25 show how much the B_{OP} maximum angle can change with respect to the offset from our ideal magnet position.

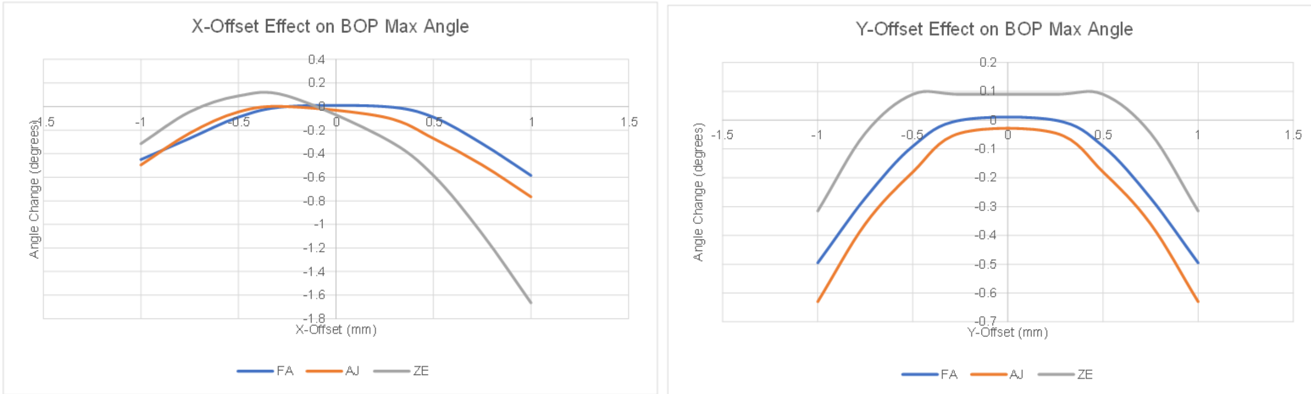

Figure 2-24. X and Y Offset Impact on B_{OP} Max Angle

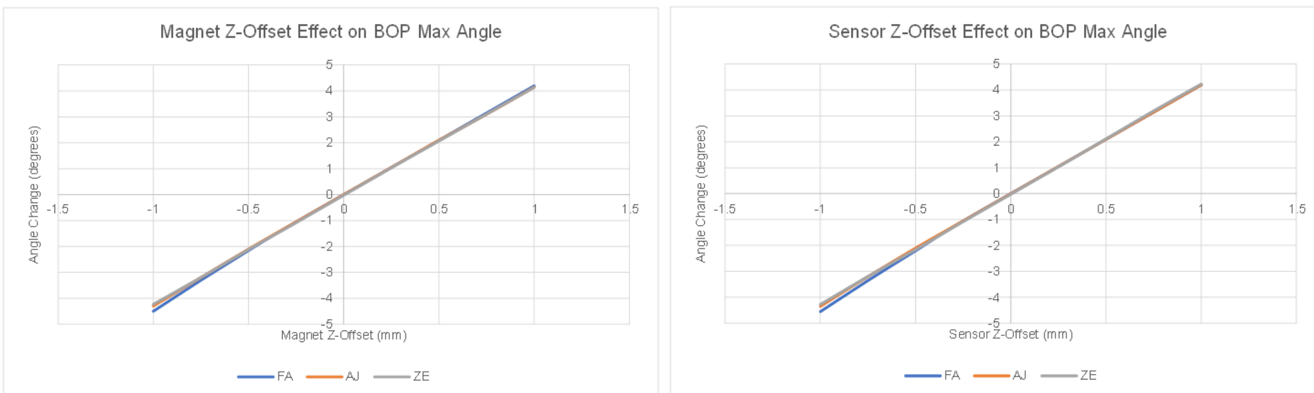

Figure 2-25. Z Offset on B_{OP} Max Angle

2.8.2 Roll, Yaw, and Pitch

Roll, yaw, and pitch correspond to how a mechanical body may be rotated away from its intended variation. In our rocker switch system, there are multiple bodies that could have some roll, yaw, and pitch. These bodies include the Hall-effect switch, the rocker base, the rocker axle, the rocker, and the magnet. Figure 2-26 illustrates roll, yaw, pitch for the magnet.

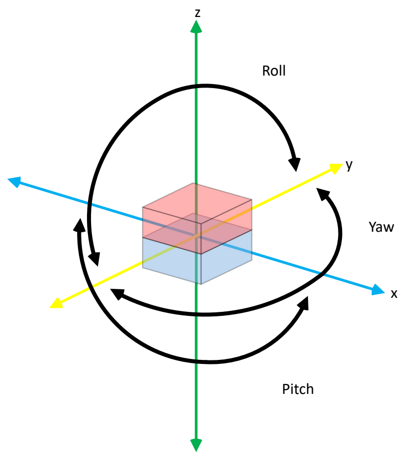

Figure 2-26. Magnet Roll, Yaw, and Pitch

Post analysis revealed that some magnets embedded in the rocker switches were not flush with the bottom of the magnet cavity. This led to some roll in the magnet orientation. Since the slots in the PCB for the rocker switch were hand drilled, those slots had tolerance that led to rocker switch yaw. Lastly as some slots were a little too large, the rocker switch had some wiggle room that resulted in some magnet pitch as well as additional offset.

The influence of magnet roll and rocker base yaw are simulated below. Tighter manufacturing tolerance with respect to the rocker switch magnet cavity and PCB slots are expected to minimize this respective error.

Figure 2-27 illustrates the impact of roll on BOP maximum angle while Figure 2-28 illustrates the impact of yaw on BOP maximum angle.

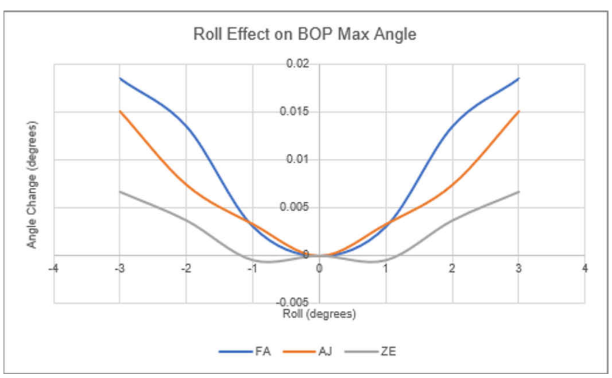

Figure 2-27. Roll Effect on BOP Maximum Angle

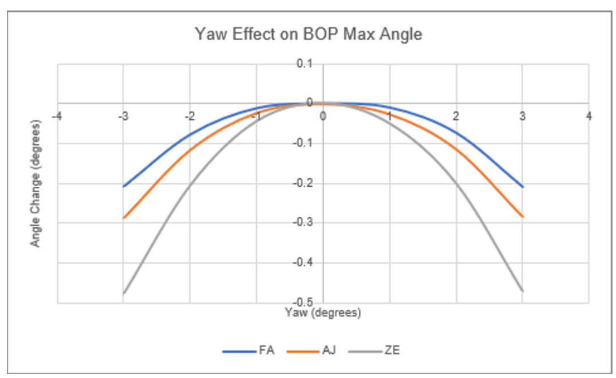

Figure 2-28. Yaw Effect on BOP Maximum Angle

2.8.3 Magnet Variation

Magnet variation comprises physical dimensions as well as material composition. This design used a block shaped magnet and the relevant dimensions include magnet length, width, and thickness. Magnet composition can vary due to impurities, and the variation in composition corresponds to a range in remanence, Br, which directly relates to field strength.

The B221 magnet used in this document has a tolerance of ±0.004 inches for all dimensions. A typical N42 magnet like the B221 has Br of 13000 Gauss. Product specifications outlined a Br maximum of 13200 Gauss, thereby suggesting a possible tolerance of ±200 Gauss.

Figure 2-29 and Figure 2-30 show how much the B_{OP} maximum angle can change with respect to the magnet variation.

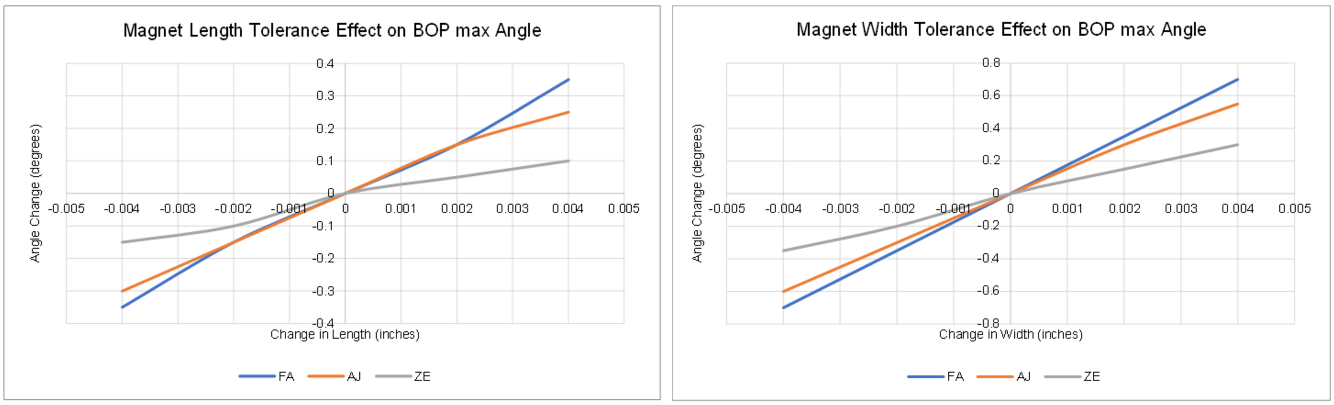

Figure 2-29. Length and Width Tolerance Impact on B_{OP} Maximum Angle

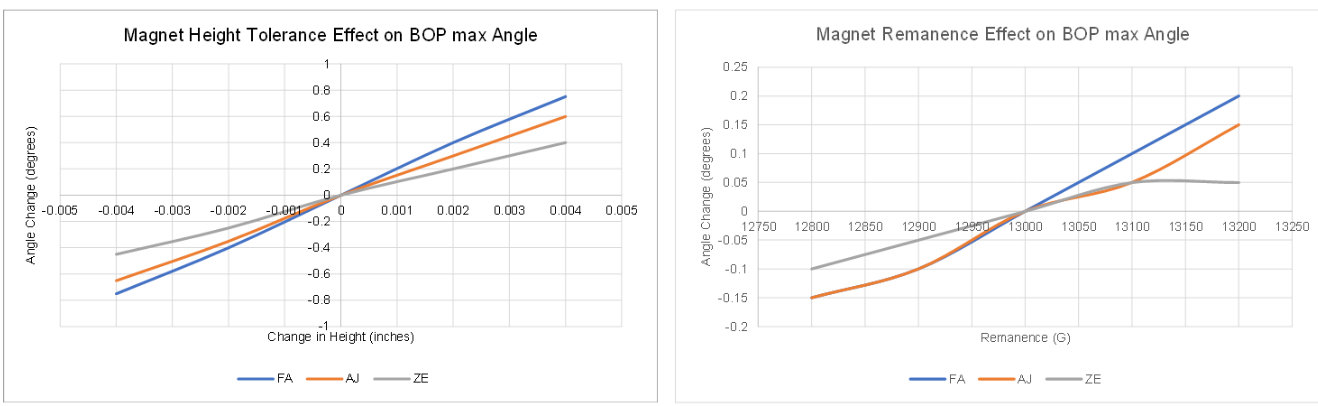

Figure 2-30. Height and Remanence Tolerance Impact on B_{OP} Maximum Angle

2.8.4 Device Variation and Temperature Drift

As previously indicated, every type of Hall-effect device, will have some manufacturing variation and its performance will drift with temperature. These issues are captured by the minimum and maximum bounds found in the data sheet as shown in Table 2-2. At a minimum these bounds should be considered in the design and are incorporated into the calculator. Smaller differences between the minimum and maximum for B_{OP} and B_{RP} will lead to much tighter designs with less variation.

Table 2-2. DRV5033 Magnetic Characteristics

over operating free-air temperature range (unless otherwise noted)

PARAMETER		TEST CONDITIONS	MIN	TYP	MAX	UNIT
DRV5033FA: ±3.5 / ±2 mT						
B_{OP}	Operate point	T_A = –40°C to 125°C	±1.8	±3.5	±6.8	mT
B_{RP}	Release point		±0.5	±2	±4.2	mT
B_{hys}	Hysteresis; $B_{hys} = (B_{OP} – B_{RP})$			±1.5		mT
B_O	Magnetic offset; $B_O = (B_{OP} + B_{RP}) / 2$			±2.8		mT
DRV5033AJ: ±6.9 / ±3.5 mT						
B_{OP}	Operate point	T_A = –40°C to 125°C	±3	±6.9	±12	mT
B_{RP}	Release point		±1	±3.5	±5	mT
B_{hys}	Hysteresis; $B_{hys} = (B_{OP} – B_{RP})$			3.4		mT
B_O	Magnetic offset; $B_O = (B_{OP} + B_{RP}) / 2$			5.2		mT

Aside from B_{OP} and B_{RP} variation, die placement and more importantly Hall-element placement can have some variation. This variation is typically found in the data sheet in a figure similar to Figure 2-31 and is equivalent to an offset error.

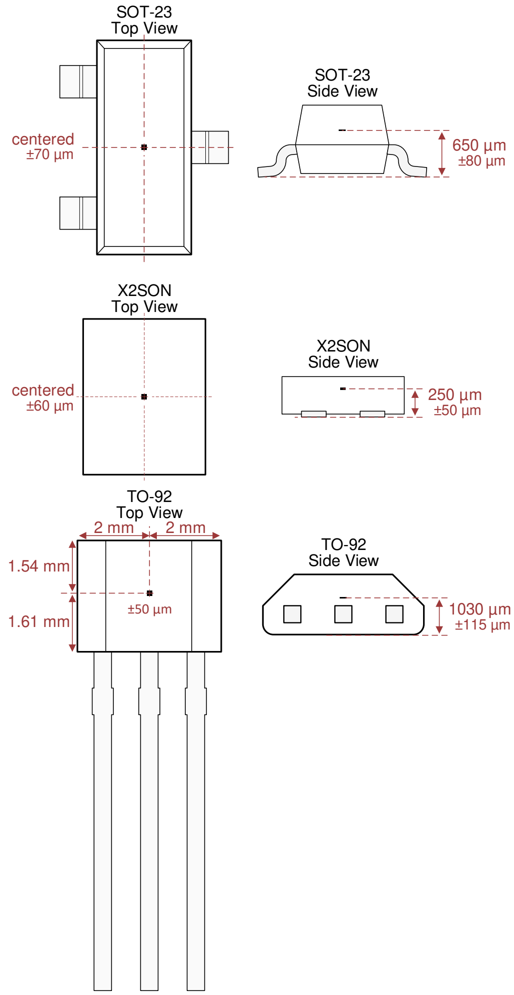

Figure 2-31. Hall Element Placement Example

2.8.5 External Fields

External fields can raise or lower the threshold angles observed in this particular design depending on the magnet orientation. One particular field that is present in nearly unshielded designs is the earth's magnetic field. This field ranges with respect to location, displacement from the earth's surface, and Hall-element orientation with respect to the earth's surface. Nearby magnets and high current carrying wires such as in a motor are also examples of external field sources. In the test environment, linear output device was used to measure an external field 42.9 µT for the board location and orientation.

One other external or stray field that is inherent to the particular design, is the field from any other magnet in one of the adjacent rockers. Figure 2-32 illustrates how much external field might be expected from a nearby rocker. As it falls well below the lowest B_{OP} minimum of 1.8 mT, this is not considered to be a significant issue in this design. However, if the rockers were spaced closer together, then it might become a significant issue for the DRV5033 devices. Shielding or using higher threshold devices should minimize this concern.

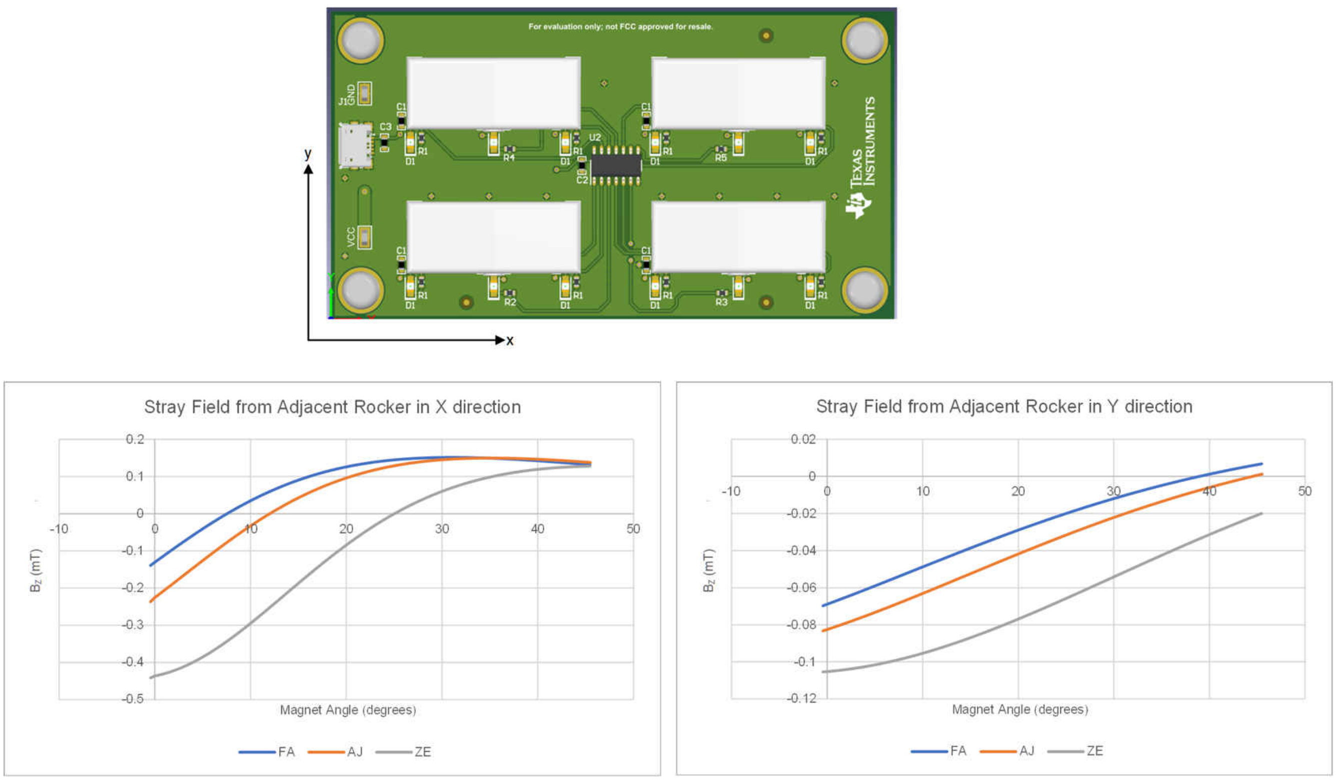

Figure 2-32. Impact of Adjacent Rocker Switches

External fields should simply offset the magnetic field curve. As illustrated in Figure 2-33, an offset that lowers the curve tightens the switch region and lower the B_{OP} angle as seen in region 1 while an offset that raises the curve leads to a wider transition region and a higher B_{RP} angle as seen in region 3. As omnipolar switches were used, strict attention was not directed to which polarity faced the device in the assembly of these rocker switches. For less variation, consistently orienting a specific polarity toward the Hall-effect switch leads to more consistent results.

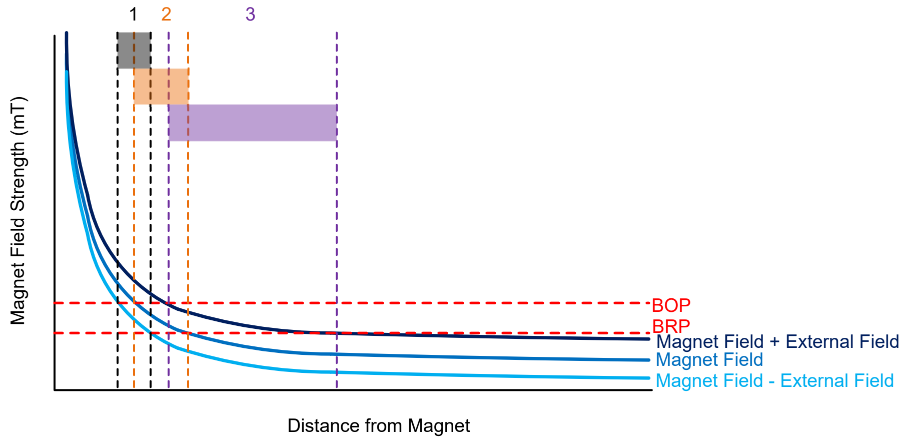

Figure 2-33. Affect of External Field

2.8.6 Nearby Material Influence

While not an expected source of error in this particular design, nearby material influence is a very important error factor to consider. In fact this possible error influenced the preliminary design approach. As previously mentioned, metal springs were intentionally avoided in the mechanical design aspect. The reason stems from the fact that many metal springs are composed of highly-permeable materials with low reluctance. Magnetic fields travel the path of least reluctance from the north to south poles of the magnet. This can either concentrate or divert your field in such a way that helps or hurts your design. When considering material influence, magnetic simulation and bench test are necessary.

To illustrate the concept of how material influences the field, Figure 2-34 shows a SOT-23 with a magnet suspended above. In the left example is a mu metal cylinder wrapping around the device. Observe that the B field concentrates within this cylinder and the aerial view of the device below illustrates that the field observed by the Hall element is basically 0 mT. By comparing to the unshielded example on the right, notice that at least 30 mT were diverted away from being measured.

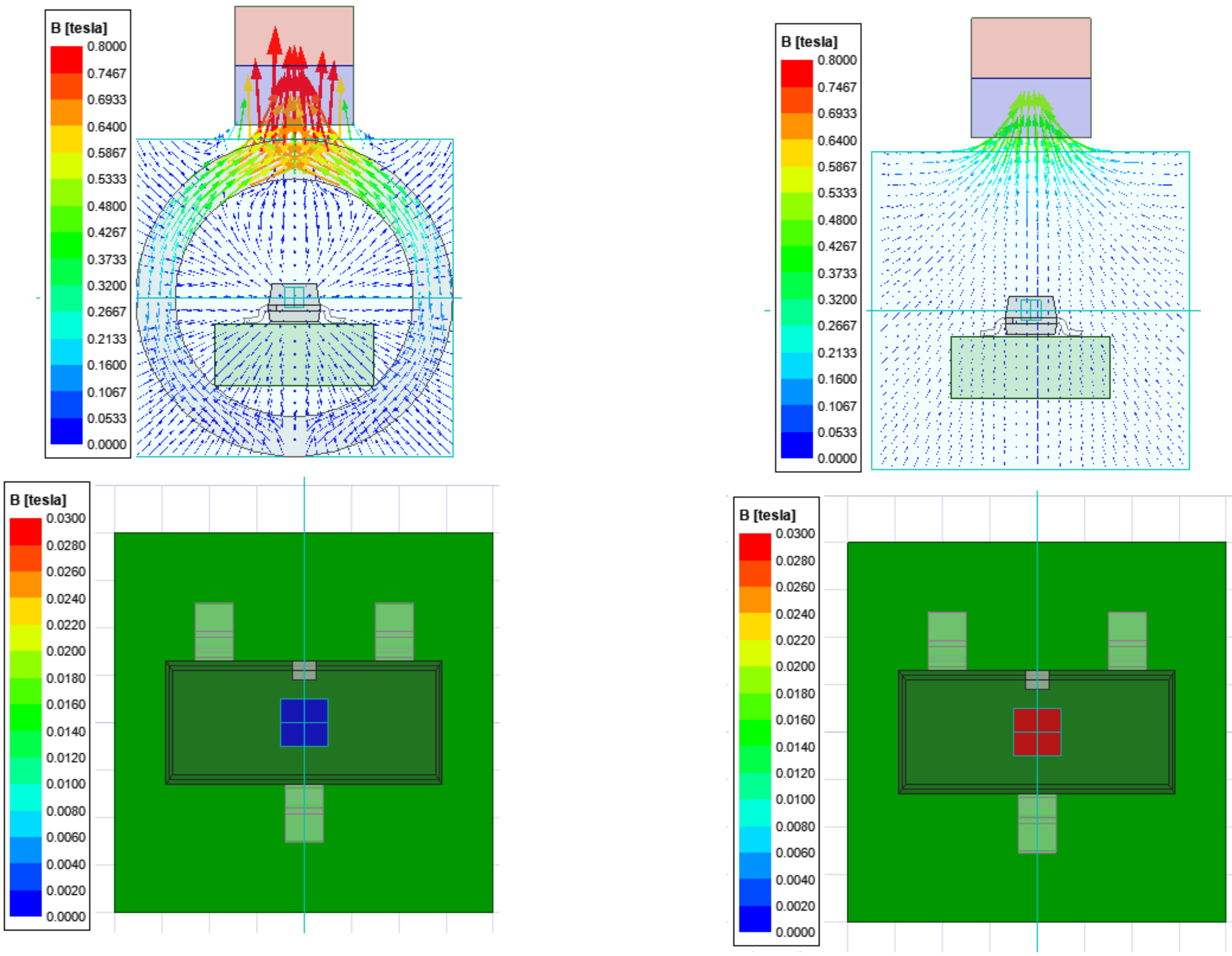

Figure 2-34. Magnet Shielding

2.8.7 Bench Setup Error

Yet another possible source of error is related to how the bench test is performed on the prototype. In this case, the rocker switch performance is assessed through video frames. The camera orientation and the resolution of the post-processing program could have affected the accuracy. Figure 2-35 and Figure 2-36 are extreme cases used to help illustrate the error. However, the errors in the assessment were significantly smaller. Figure 2-35 shows how the base used for calculation has some pitch from the actual base. The right image in Figure 2-36 shows how some yaw with respect to the viewing angle leads to a larger measurement angle when both rockers are in the same default position.

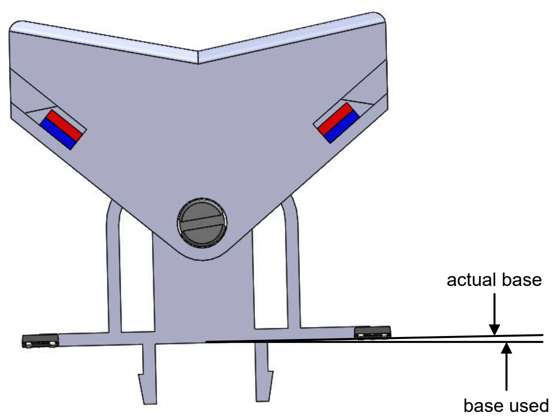

Figure 2-35. Image Pitch

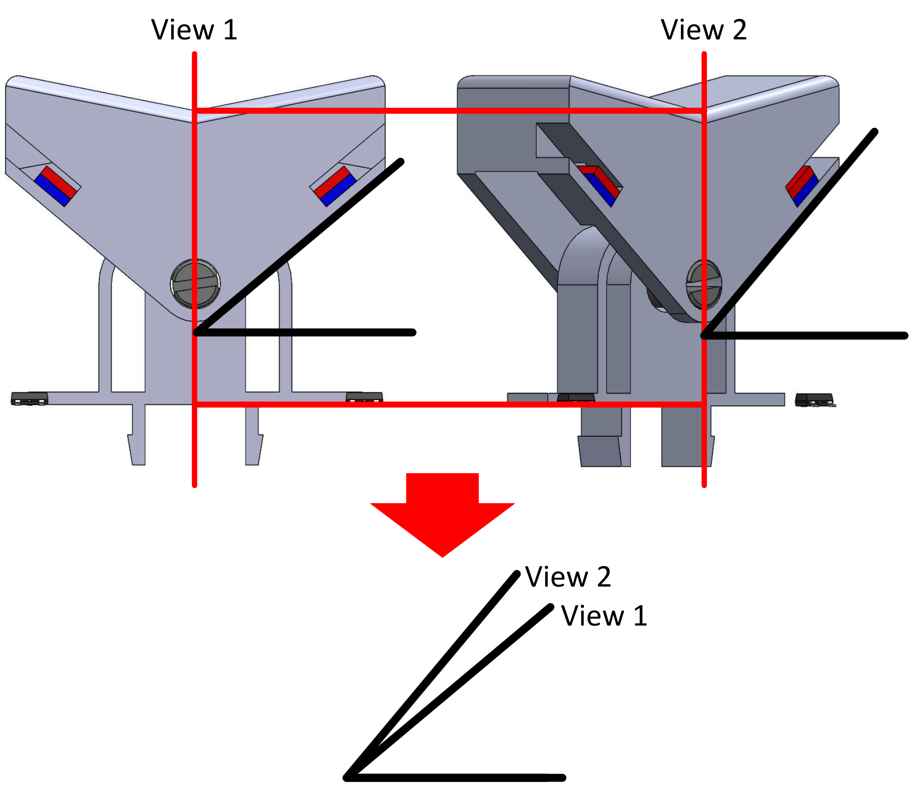

Figure 2-36. Captured Body With Yaw

3 Summary

This application report covered the process for designing a rocker switch with Hall-effect sensors. This process started with covering the basic implementation of the rocker and progressed through selecting a device based upon calculations performed in the Magnetic Sensing Proximity Tool. After the preliminary theoretical design process, prototyping and bench measurement were covered. From the bench measurement section, this report stressed that there are other sources of error besides device variation. Basic error analysis for each possible source was then presented.

Mailing Address: Texas Instruments, Post Office Box 655303, Dallas, Texas 75265